Discover Sustainability

RESEARCH

Open Access

Insight for sustainable supplemental irrigation development for Cocoa in changing Ghana's agroforestry landscapes

Seifu A. Tilahun[1], Andoh K. Amponsah[1], Gerald Atampugre[1*], Birhanu Z. Birhanu[1], Moctar Dembélé[1], Sylvester Darko[4], Tafadzwanashe Mabhaudhi[2,3] and Olufunke Cofie[1]

*Correspondence:
Gerald Atampugre
g.atampugre@cgiar.org
[1]International Water Management Institute, PMB CT 112, Airport Residential Area, Accra, Ghana
[2]International Water Management Institute, 333 Grosvenor St, Hatfield, Pretoria, South Africa
[3]Centre for Transformative Agricultural and Food Systems, University of KwaZulu-Natal, Pietermaritzburg, South Africa
[4]Ghana Hydrological Authority, Accra, Ghana

Abstract
Cocoa production in Ghana faces challenges from climate change and land use dynamics, necessitating sustainable intensification through supplemental irrigation. However, the availability of water resources for irrigation remains underexplored in Ghana's agroforestry landscapes. This study assesses the potential of water resources for irrigation and impacts of land use and climate changes in the moist semi-deciduous agroforestry-dominated Upper Offin basin. Using Landsat images, the study analyzed land use patterns, hydro-climatic trends (1981–2022), and water balance based on rainfall and evapotranspiration. Findings reveal that streamflow represents only 10% of average annual rainfall (1333 mm), with subsurface flow predominating. Annual actual evapotranspiration (AET) accounts for 85% of rainfall, while deep percolation offers additional water potential. Shallow groundwater could irrigate 10% of the area during the 5-month dry season, doubling with deep percolation. Land use changes threaten this potential, as forest areas declined while cropland and grassland expanded (2008–2021), associated highly with the alteration of water balance components. Although rainfall remained stable, rising temperatures could increase cocoa water demand. AET declined over time, correlating with FAO-WaPOR data, while streamflow increased during the observed period (1986–2012). The study recommends groundwater supplemental irrigation systems for sustainable cocoa farming in Ghana and similar agroforestry regions, addressing climate and land use challenges effectively.

Keywords Water balance, Land use, Irrigation, Remote sensing, Cocoa, Ghana

1 Introduction
The rapid population growth in Africa, projected to reach over 2 billion by 2050 [1], is expected to put immense pressure on the continent's agri-food system. This surge in population, coupled with the increasing demand for food, has led to the expansion of agricultural land twofold in the last two decades [2], often at the expense of natural habitats and the environment [3]. Current changes in land use practices, such as converting forests into agricultural areas, are intensifying pressure on surface and groundwater

resources [4]. Furthermore, these challenges are exacerbated by climate change, which has a multiplier effect on all of these drivers, making the situation dynamic and even more complex to address [5].

Securing and sustaining Africa's agricultural production requires innovative and sustainable land management practices, climate-smart technologies, climate information services, and a realignment of policy and finance to increase investment in agribusiness [6]. One of the adaptation mechanisms for boosting agricultural production in a changing climate and landscape is sustainable intensification through supplemental and dry-season irrigation [7].

However, to effectively implement such adaptation strategies, a comprehensive understanding of the land use system and the temporal and spatial availability of water in the region is essential. A comprehension of recent trends in climate, land use patterns, and water balance assessment is essential for evaluating the distribution of water resources across the landscape, tracking their temporal fluctuations, and evaluating how they are impacted by climate change and land use patterns [8, 9]. A major challenge facing sub-Saharan Africa in environmental monitoring and resource management is the paucity of reliable, high-resolution, and long-term ground-based data [10]. This data scarcity hinders comprehensive assessments of climate trends, land use dynamics, and water balance. In this context, remote sensing emerges as a powerful tool, offering consistent, scalable, and timely datasets that can bridge the information gap. This analysis provides the necessary information and insight to formulate sustainable irrigation strategies and make informed decisions on water resource management. Such an approach ensures that agriculture can thrive while preserving the environment and addressing the challenges posed by a changing climate and a growing population [7].

Cocoa is the backbone of Ghana's economy as a key export agricultural crop and an essential livelihood for smallholder farmers [11, 12]. However, the reliance on rainfed systems in cocoa production is increasingly challenging due to changes in rainfall patterns, consecutive dry days and rising temperatures [13]. The stress on water resources jeopardizes cocoa yields and threatens the livelihoods of smallholder farmers, who comprise the majority of producers [14]. There has been growing interest in adopting supplemental irrigation for cocoa farming in response to these challenges. The Ghana Cocoa Board (COCOBOD), supported by government and donor agencies, aims to enhance resilience and productivity in the face of climate uncertainties [15, 16].

Although water resources for irrigation have been assessed at continental and national scales [17, 18], more studies are needed at the sub-national level to improve planning of supplemental irrigation interventions in cocoa-producing areas. For instance, irrigation is one strategy to close the water deficit of about 50% of the cocoa yield gap. As a result, the COCOBOD and various private sector actors have trailed solar-powered irrigation pumps with drip system [19]. Such irrigation interventions have increased cocoa yields by 60% compared with farms under only rainfed agriculture [20]. Gbodji et al. [21] identified a strong interest in solar-based irrigation in cocoa by Ghanaian cocoa farmers. However, studies lack the water resources' potential for specific locations in cocoa-producing areas [22].

A recent investigation by Akpoti et al. [23] in the cocoa-growing region has identified the groundwater potential for cocoa. However, this study primarily relied on GIS and remote sensing techniques, lacking a quantitative assessment of water resources. The old water balance studies in the early 2000s have shown that evapotranspiration amounts to approximately 1200 mm, with deep percolation accounting for 17% of rainfall [9]. In the same region, other studies, such as Awotwi et al. [8], have utilized SWAT modeling to assess the impact of land use changes within the Pra-basin. Additionally, research conducted by Boakye et al. [24] has analyzed climate trends and land use/cover changes in the Pra River Basin, while Awotwi et al. [25] focused on the influence of mining activities on water balance components. These studies highlight the need for further research on cocoa-producing areas that consider the unique water resource dynamics at smaller scales, as these variations can significantly impact irrigation planning and sustainable water management in cocoa-producing regions.

In these areas, anthropogenic activities mainly contributed to increased runoff [8, 25]. The main anthropogenic changes in the area are related to land use changes like small-scale mining (usually illegal), excessive lumbering, and increased crop farming. Between 1986 and 2016, cropland expansion, settlements, and mining led to increased surface runoff and water yield [8]. In 2015, the cocoa-growing region's total Galamsey (local name for illegal mining) extent reached 43,879 hectares, causing downstream pollution [26]. Galamsey operations expanded along major river networks like the Pra and its sub-basin Offin, increasing surface runoff and baseflow, while large-scale activities decreased runoff and increased baseflow [27].

As Ghana increasingly focuses on transforming cocoa farming through irrigation, it is imperative to assess changes in land use practices and historical climate trends. Understanding how these changes affect water resource availability in agroforestry-dominated landscapes is crucial. Previous studies have either mapped irrigation potential or tracked land use changes in cocoa-producing regions. In contrast, this study integrates long-term hydro-climatic trends with a conceptual hydrological model to assess the potential for supplemental irrigation in a cocoa agroforestry landscape. By quantifying the contribution of subsurface flows, evapotranspiration losses, and deep percolation, we move beyond potential mapping to evaluate the feasibility of dry-season irrigation [8].

This study, therefore, aims to estimate the available water resources for supplemental irrigation of cocoa farms and the potential threats of land use and climate change to the water availability in the moist-semi deciduous agroforestry-dominated landscape of the upper Offin basin, Ghana. This study is therefore outlined by first calculating the different water balance components of the Upper Offin Sub-basin using a conceptual water balance model and then estimating its irrigation potential. Then the study presents the changes in land use and land cover and historical climate changes as threats to water availability. Finally, it presents evidence of how land use and land cover changes could bring change in water availability in the basin.

2 Materials and methods

2.1 Description of the study area

The study area, Upper Offin (at the Adiembera hydrological station), is situated in the upper part of Pra River Basin, the southern part of Ghana (Fig. 1). The Upper Offin watershed can be located 6°40′0″N 2°10′0″W and it covers an area of 3070 km^2, draining directly to Offin River (See Fig. 1), one of the major tributaries of the Pra River basin. It falls within the sub-equatorial wet climate zone with two rainy seasons (March to July and September to November). It is humid throughout the year, with an average

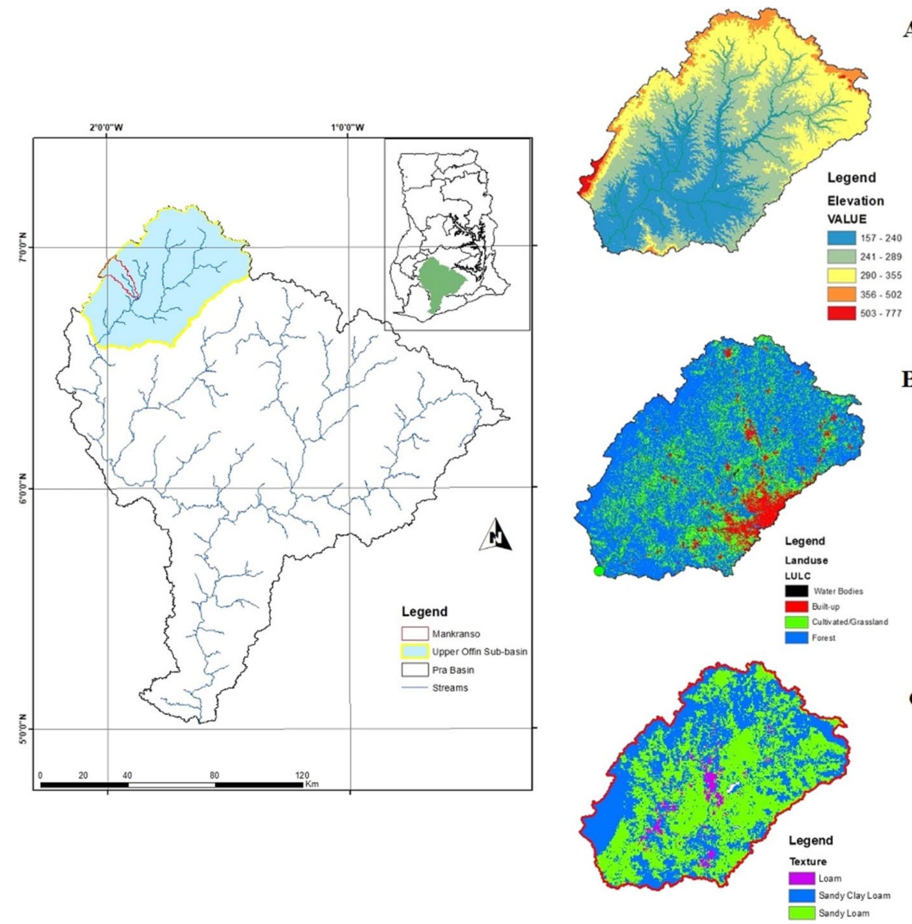

Fig. 1 Location of upper Offin within Pra River Basin and Mankran watershed in the upper Offin, Elevation (**A**), Land use and cover (**B**) and Soil texture (**C**) maps of the upper Offin sub-basin

temperature ranging from a minimum of 22˚C in August to a maximum of 32˚C in March. The average annual rainfall is 1350 mm, between 1000 and 1700 mm. The watershed has a Bio-modal rainfall pattern with a sub-humid climate with an average annual rainfall of 1350 mm.

2.1.1 Elevation and geology

The elevation of the upper Offin (Fig. 1A) varies within the ranges of 157 to 777 m asl. The watershed peaks at upslope, and the landmass slopes down from the upland towards the watershed outlet. About 58% of the area lies within the slope range of 0–8.5% and 37% within 8.5 to 20%, which are generally classified as flat to undulating to hilly topographic features. The area is dominated by early Proterozoic crystalline rocks collectively known as the Birimian and Tarkwaian rocks, with ages ranging between ~ 2.31 and 2.06 Ga [28]. Much of the gold occurs in the Palaeoproterozoic Birimian Supergroup and Tarkwaian Group, which comprise Ghana's southwest to northeast Birimian belts [29]. Such formations in the area generally fall within the medium water yield (30 – 60 $lmin^{-1}$) and high-water yield (> 60 $lmin^{-1}$) zones and have a specific capacity range of 0.21 – 99.65 m^2day^{-1} [30].

2.1.2 Soil
The main soil type found in the study area is acrisols, which constitute more than 90% of the study area, and the remaining area is leptosols [8]. According to the USDA soil map classification [31], the soil texture of the Upper Offin sub-basin (Fig. 1C) is dominated by sandy clay loam (46%) in the upper slope and sandy loam (51%) in the middle and the valley bottom. The upslope soil is well-drained, and the area's maximum available water content is estimated at 200 mm within the root zone [9].

2.1.3 Land use and farming system
The land use land cover (LULC) from the European Space Agency World Cover 10m, 2020 product [32] is shown in Fig. 1B. The dominant land uses are forests (~ 66%) with dense vegetation, planted cropland and grassland (~ 28%) and built-up areas (~ 6%). The area is moist-semideciduous forest vegetation, home to most of Ghana's valuable timber trees and cocoa farming. Due to the rapid expansion of cocoa plantations (> 50% of the forest), only a small portion of the native forest vegetation remains, resulting in the dominant secondary vegetative cover [33, 34].

The study area is dominated by smallholder farmers engaged in agroforestry, predominantly cocoa farming in upland forest areas, alongside the cultivation of rice and vegetables in the valley bottom and mining. The major crops cultivated in the area also include cereals such as corn, tree cash crop plants such as oil palm, bananas, cassava, and plantain. The average landholding of cocoa farms in the area is 3.0 hectares. The area contains the highest density of settlements (both rural and urban) in Ghana. It has a high concentration of mining activities, mainly focused on gold and other minerals [35]. A closer examination of land-use change patterns is conducted within the upland Mankran watershed in the upper Offin, representing a micro-watershed of the broader sub-basin.

2.2 Framework of the study
A methodological framework, shown in Fig. 2, was used to estimate the available water resources for supplemental irrigation of cocoa farms and the potential threats of land use and climate change to water availability in the moist-semideciduous agroforestry-dominated landscape of the upper Offin basin, Ghana.

For sustainable supplemental irrigation planning in Ghana's cocoa agroforestry systems, multiple hydrologic models offer distinct advantages. Physically based tools like the Soil and Water Assessment Tool (SWAT) [8] and Soil and Water Integrated model (SWIM) [36] provide semi-distributed simulations of soil moisture, ground water recharge, and runoff, but require extensive climatic, soil map, and parametrization of soil layer, land-use data, and crop management data, which are often scarce in Sub-Saharan Africa. In contrast, the Thornthwaite Mather water balance (TM-WB) model [37–39], applied in this study, offers a parsimonious, conceptual framework to estimate key hydrologic fluxes, including actual evapotranspiration, baseflow, and overland runoff, using minimal inputs (rainfall and temperature-based potential evapotranspiration). Its low data requirements and calibration efficiency with streamflow data make it ideal for initial assessments in data-limited areas such as the Upper Offin sub-basin. By classifying the watershed into hydrological response units and estimating surface/groundwater availability, TM-WB provides an understanding of irrigation potential during dry periods and guides targeted field studies for parametrization of soil and crop management

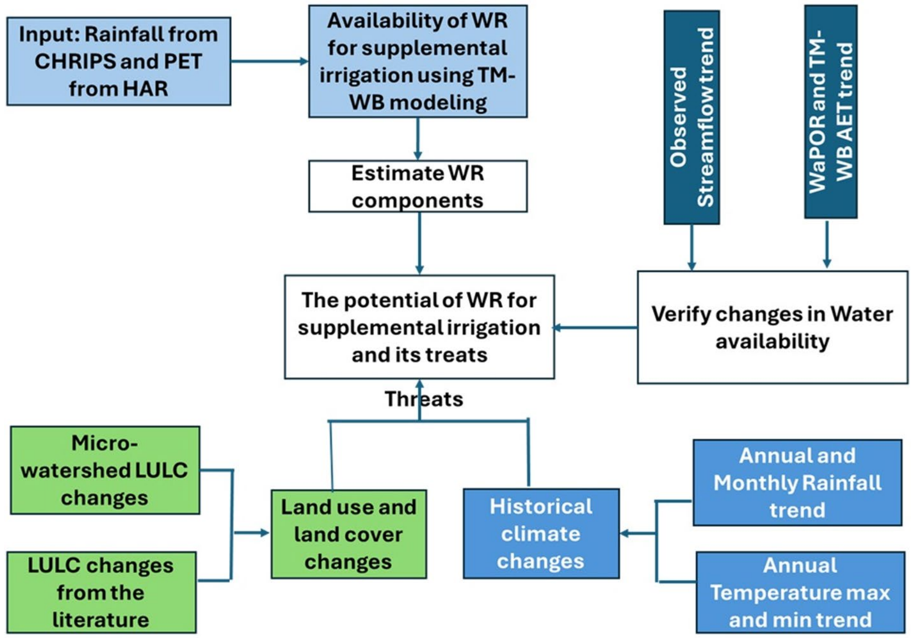

Fig. 2 Flowchart used to achieve the objective of the study. CHIRPS stands for Climate Hazards Group Infrared Precipitation with Stations, HAR is for Hargraves method, WR is water resources, TM-WB is for Thornthwaite Mather water balance, and AET is actual evapo-trnaspiration

data needed by models like SWAT and SWIM. This pragmatic choice aligns with the study's goal of generating rapid, actionable insights for smallholder farmers while balancing technical feasibility and resource constraints in Ghana's cocoa landscapes.

To evaluate land use and land cover (LULC) changes, a representative micro-watershed, Mankran, was used to map historical land uses in 2008, 2015, 2018, and 2021. Literature LULC changes in Upper Offin were used to compare the results [24]. To evaluate historical climate change, the Mann–Kendall trend test of annual precipitation, monthly precipitation, annual maximum temperature, and minimum temperature was conducted. As evidence of how land use changes affect water availability, a Mann–Kendall trend test was conducted using observed streamflow data and actual evaporation estimates from a WaPOR remote sensing product and TM-WB model. The following sections describe in detail the methodology.

2.3 Estimating water resources potential for supplemental irrigation

2.3.1 Thornthwaite Mather's water balance modeling

Thornthwaite Mather's water balance modeling (TM-WB) was employed to estimate the components of the water balance, including surface runoff, subsurface flow from baseflow, actual evaporation, and recharge. The TM technique has been effectively employed in African watersheds and basins [37, 40]. The Parameter Efficient (Semi)-Distributed Water Balance Model (PED-WM) based on Thornthwaith Mather was adopted. The model has been widely applied in the sub-humid upper Blue Nile basin [37–39]. One can find the general framework of the model in Tilahun et al., [39] and Alemie et al. [41]. This modeling framework was adapted for this landscape.

The water balance model used precipitation and potential evapotranspiration data as input from remote sensing and in-situ secondary data reanalysis from 2001 to 2012 because of observed data availability (Table 1). Daily precipitation from 1981 to 2021 was obtained from CHIRPSv2.0, as explained above. Potential evapotranspiration was calculated using the Hargreaves (HAR) method, which requires daily maximum and minimum air temperatures, and extraterrestrial solar radiation computed from the study site's latitude. The Hargreaves and Samani [42] equation is defined as follows:

$$ET_0 = 0.0023\,(T_{max} - T_{min})^{0.5}(T_{mean} + 17.8)Ra \tag{1}$$

where T_{min} is the daily minimum temperature [°C], T_{max} is the daily maximum temperature, T_{mean} is the mean temperature and Ra is extraterrestrial radiation [MJ m^{-2} day^{-1}].

Observed monthly streamflow at Adimbera station from 2001 to 2012 was used to calibrate and validate the model using parameters defined in Table 1. The performance of the calibrated TM-WB model in predicting monthly streamflow during the calibration and validation period was evaluated using commonly used statistics, R-squared (R^2), Root mean squared error (RMSE) and Nash–Sutcliffe Efficiency (NSE). The TM water balance module was calibrated using monthly data from 2000 to 2005 at Adiembera station in the upper Offin subbasin. The time step followed was monthly, and validation was carried out for the period from 2006 to 2012.

The selection of the model was also based on the assumption (Table 2) that the TM-WB model is suitable to simulate the Upper Offin landscape with a sub-humid monsoonal climate and its ability to divide the landscape into a number of conceptual landscape units [37, 40]. The landscape in the study area has a depressed area or valley bottom lying at the lowest position in the landscape and an elevated area with relatively high permeability and good drainage status compared to the rest of the landscape [43]. Therefore, the upper Offin landscape is divided into three units with different soil moisture conditions in the model. The model configuration was also used to simulate and

Table 1 Input parameters and data for calibration and validation of the Thornthwaite-Mather Water Balance (TM-WB) Model

Parameters/Input data	Symbol	Description	Unit	Sources
Saturated area fraction	A_s	Portion of the valley bottom saturated area	%	Calibration with streamflow at Adiembera station
Hillside area fraction	A_h	Portion of the hillside contributing to the flow	%	Calibration from streamflow data
Soil moisture storage (saturated area)	$S_{max,s}$	Maximum soil water storage in the saturated zone	mm	Based on literature [9] and calibration with streamflow
Soil moisture storage (hillside)	$S_{max,h}$	Maximum soil water storage in the hillside area	mm	Calibration with streamflow
Baseflow reservoir storage	B_{smax}	Max storage for baseflow reservoir	mm	Calibration with streamflow
Baseflow half-life	$t_1/_2$	Time for baseflow decay	days	Calibration with streamflow
Interflow travel time (hillside)	τ_h*	Time for water to reach the outlet via the hillside interflow	days	Calibration with streamflow
Interflow travel time (saturated area)	τ_s*	Time for water to reach the outlet via the saturated area	days	Calibration with streamflow
Potential Evapotranspiration	PET	Estimated using Hargraves' equation	mm day^{-1}	ERA5 bias-corrected temperature data (1980–2022)
Precipitation	P	Reanalysis product	mm day^{-1}	CHIRPSv2.0 (1981–2022)
Streamflow	Q	Observed flow	mm day^{-1}	Adiembera station data provided by Ghana Hydrological Authority

Table 2 Assumptions and references used in the TM-WB model, and irrigation potential estimations

Assumptions	Details	Reference
Model structure	Watershed is divided into three hydrological zones: runoff, interflow, and non-contributing	Tilahun et al. [39], Alemie et al. [41] and based on local landscape description by Obalum et al. [43]
Soil moisture storage	Storage values based on USDA classification and field capacity	Christiansen and Awadzi [9]
Effective rainfall method	USDA-SCS method	Allen et al. [51]
Water use efficiency	60% irrigation application efficiency	Sekyi-Annan et al. [48]
Net irrigation requirement	525 mm/year during dry season	[50]); stakeholder engagement [16]
Minimum ecological flow	90-percentile streamflow used as ecological threshold	Worqlul et al., [49]

extend the observed streamflow from 2012 to 2022. The new simulated flow rate was then utilized to determine the landscape's irrigation potential.

The first unit contributes to runoff through quick interflow, the second to subsurface flow via interflow and baseflow, and the last unit does not directly contribute to the outlet but is lost through deep percolation or actual evaporation, which is not directly calculated in the model. In this study, we modeled the first unit as a quick interflow-producing area and the second unit as one with high-permeability area that infiltrates precipitation. The infiltrated water recharges two types of subsurface reservoirs: a zero-order reservoir, which is a shallow, quick-draining zone that contributes to interflow (lateral subsurface flow); and a first-order reservoir, which is a deeper, slower-draining zone that sustains baseflow (long-term groundwater discharge to streams). The main limitation of the model is that it cannot explicitly define the spatial locations of these units; instead, it defines them implicitly based on the partition of the flow to different components and landscape positions.

For the three areas, the water balance is calculated for the root zone:

$$AW_t = AW_{t-\Delta t} + (P_t - AET_t - q_t)\,\Delta t \tag{2}$$

where at time t, P_t is the precipitation, AET_t is the actual evapotranspiration rate, AW_t is the available water in the root zone per unit area and q_t is either the surface runoff for the upland area or the percolation out of the root zone that recharges the aquifer. The actual evaporation AET_t is calculated with Eq. 3.

$$\mathrm{AET}_t = e_{p_t} for p_t \geq e_{p_t} \tag{3a}$$

$$\mathrm{AET}_t = \frac{AW_{t-\Delta t}}{\Delta t}\left[1 - \ \exp\frac{(p_t - e_{p_t})\,\Delta t}{AWC}\right] \mathrm{for} p_t < e_{p_t} \tag{3b}$$

where e_{p_t} is the potential evapotranspiration and AWC is the available water capacity of the soil in the root zone.

The excess water above field capacity would be either the surface runoff (q_t) for the upland area or the percolation out of the root zone that becomes recharge to the aquifer or interflow or deep percolation (r_t). Deep percolation is part of recharge that does not contribute flow to the outlet and is considered unaccounted for. Recharge is calculated by Eq. 4.

$$r_t = \max[[AW_{t-\Delta t} + (p_t - \mathrm{AET}_t)\,\Delta t - AWC]\,, 0] \tag{4}$$

Part of the percolation that reaches the aquifer becomes baseflow (q_b) and expressed by Eq. 5 as a linear reservoir that exponentially decreases flow in time with the baseflow flow storage at time t (BS_t) and specific half time ($t_{1/2} = 0.69/\propto$).

$$q_b = \frac{BS_t\,(1 - \exp(-\propto \Delta t)}{\Delta t} \tag{5}$$

The work of Alemie et al. [41], predicting shallow groundwater tables for sloping highland aquifers was used to compute the interflow (q_i)flow by averaging the percolation over time, τ*, which is the time required for water to flow from the most distant point in the landscape unit to the point of interest (e.g., stream outlet). This is calculated by Eq. 6.

$$q_{i,t} = \frac{\sum_0^{\tau^*-1} r_t}{\tau^*}\text{for}\tau \leq \tau^* - 1 \tag{6}$$

The model has nine main parameters (Table 1), including the area fraction (*A*) and the maximum storage capacity (S_{max}) for the three zones and three subsurface parameters: the half-life ($t_{1/2}$) to describe the exponential decay in time and maximum storage capacity (B_{Smax}) of the first-order reservoir and the drainage time of the zero-order reservoirs (τ*), which describes a linear decrease in time for the interflow. A detailed description of the model can also be found in Alemie et al. [41].

2.3.2 Data Collection

Precipitation and temperature were sourced from remote sensing products and the Ghana Meteorological Agency (GMet). GMet provided daily minimum and maximum temperature measurements for Kumasi stations from 1980 to 2016. Rainfall data for the same period was challenging to get from GMet. As a result, a retrieved reanalysis product for precipitation was obtained from Climate Hazards Group Infrared Precipitation with Stations (CHIRPSv2.0 with 0.05° resolution) [44]. The CHIRPS data was used because of its ability to represent the seasonal rainfall patterns and analyze all extreme events in Ghana [45]. While CHIRPS' spatial resolution of 0.05° (approximately 5 km) provides reasonably high coverage for regional analysis, it may introduce uncertainties when applied to a highly localized scale, potentially affecting local-scale accuracy. The spatial daily average rainfall from 1981 to 2022 in the upper Offin sub-basin was computed using the Google Earth Engine (GEE) platform. These values were used in the TM-WB model and for trend analysis in Sect. 2.4.

For *temperature*, the European Community Medium-range Weather Forecasts v5 (ECMWF-ERA5) [46], NOAA-Climate Forecast System Reanalysis v2 (CFSR) [46], and NASA-MERRA v2 Modern Reanalysis [47] were used to select the relatively better product. The selection was based on the type of product that yields a better coefficient determination and mean bias compared to the observed temperature from 1980 to 2016. Validation of ECMWF-ERA5, CFSR, and MERRA Reanalysis satellite products for temperature showed that the maximum temperature data of ERA5 (R2 of 0.72, and mean bias of – 0.72 °C) outperformed the other products. Similarly, for minimum temperature, ERA5 resulted in R^2 of 0.5 and a mean bias of 0.24 °C). For the other two products, CFSR (R^2 of 0.5, mean bias of 1.42 °C) and MERRA (R^2 of 0.56, mean bias of -0.76 °C) became the performance while CFSR (R^2 of 0.25, mean bias of -1.43 °C) and MERRA (R^2 of 0.3, mean bias of -0.54 °C) were the performance for minimum temperature. A bias correction for the ERA5 product was selected and used to estimate the daily spatial average minimum and maximum temperature from 2017 to 2022 for the study area using the GEE platform. These were used in the Hargraves (HAR) method to estimate PET. For the trend analysis in Sect. 2.4, the bias-corrected data from 1980 to 2022 were used.

The water balance model used streamflow data for calibration. Daily river discharge at Adiembera station in the upper Offin sub-basin was obtained from the Ghana Hydrological Authority. Daily streamflow data were from May 1957 to June 2012. Missing values constituted 32 percent of the data. The period from 2000 to 2012 was used to calibrate (2000–2005) and validate (2006–2012) the model at monthly time scales. The monthly scale was chosen to minimize errors associated with the indirect measurement of precipitation from remote sensing, and the goal of the modeling was to estimate seasonal water availability. The calibrated model was then used to simulate the flow at Adimbera station from 2012 to 2022, and these simulated data were used to estimate the irrigational potential. The data from 1957 was only used to observe the general trend of streamflow.

2.3.3 Potential for supplemental irrigation

Cocoa irrigation is not widely practiced in Ghana. For this analysis, we assumed the use of surface water through furrow irrigation during the dry season (November to March) as outlined in Table 2. This assumption was made to provide a conservative estimate of the potential irrigable area, acknowledging that more efficient methods like drip or sprinkler irrigation could support greater coverage. A water application efficiency of approximately 60% was used, based on Sekyi-Annan et al. [48], to calculate the gross irrigation requirements. The study acknowledges that irrigation efficiency varies by regions (evaporation rates), crops (water requirements), soil type (water holding capacity), and irrigation technology and management practices (application uniformity), and proposes further field studies for cocoa.

The irrigation potential proportional area during average flow, maximum flow, and low flow was computed as the quotient of the long-term monthly average, maximum, and low flow depth, and the net irrigation requirement. This proportional area represents the fraction of the sub-basin that can be irrigated under specific flow scenarios. The average flow depth was derived from the mean monthly river discharge between 2012 and 2022, expressed as depth over the study area. Maximum flow depth referred to the highest observed monthly mean discharge during this period, while the low flow depth represented conditions where flow is exceeded 90% of the time, indicating scenarios of limited water availability [49].

To compute this flow, the exceedance probability was first computed and plotted against the daily streamflow discharge. The net irrigation requirement, the total water that must be supplied through irrigation to meet a crop's water demand (Allen, 1998), for surface water overflow irrigation was calculated by deducting effective rainfall from the average gross irrigation requirement (130 mm per month) for cocoa farming. This is calculated based on the cocoa transpiration rate of 4.2 mm day^{-1} [50]. Cocoa is considered because of its dominance in the landscape and the current surge in interest in irrigation for cocoa by the Ghana Cocoa Board [16]. The effective rainfall (Pe) was computed using the United States Department of Agriculture Soil Conservation Service (USDA-SCS) method [51] as shown in the equation below.

$$\left(\begin{array}{l} Pe = 0.8xP - 25P > 75\mathrm{mm/month} \\ Pe = 0.6xP - 10P < 75\mathrm{mm/month} \end{array} \right) \tag{6}$$

The annual recharge that becomes baseflow from the water balance model was used as readily available groundwater for irrigation. The potential irrigable land, estimated as a percentage of shallow groundwater recharge, was computed as the annual average baseflow divided by the net irrigation requirement. The study area is underlain by Birimian crystalline rocks [28] and recharge is usually in the form of direct precipitation through the fracture and fault zones along the hillsides [52].

2.4 Evaluating threats from LULC and climate change

2.4.1 Land use land cover changes in the mankran watershed

In a representative upland micro-watershed of Mankran, LULC analysis was done from 2008 to 2021. This analysis compared the changes in the upper Offin sub-basin reported by [24] with the Mankran watershed.

Historical images of the Mankran watershed were obtained from Google Earth for the years 2008, 2015, 2018, and 2021, with 2008 serving as the base year. All the images obtained to reduce the cloud effect were taken in January, except for the 2021 image, which was taken in December. The images were georeferenced using the ArcGIS software. The land use and cover were classified into five categories: cultivated (including cash crops and subsistence farming), forest (encompassing all-natural vegetation), built-up areas (including artificial surfaces), degraded areas, and mining sites, as well as water bodies. The field data collection, such as participatory resources mapping (PRM) in 2022 by Atampugre et al. [53], gave insight into the LULC classification.

One hundred seventy-eight (178) training samples covering all land use land cover classes were purposefully collected from the watershed to aid the interpretation. Segmented images were created from the object-based classification process. The derived image and 110 stratified and randomly selected training samples were used to identify and classify land use & land cover types. Specifically, object-based image classification with the Support Vector Machine algorithm was used [54]. The proportion correctly classified (PCC) index and the Kappa statistic, derived from an error matrix, were used to measure classification accuracy.

2.4.2 Historical climate change using trend analysis

To evaluate historical climate change, the annual and monthly maximum and minimum temperatures, as well as precipitation, were analyzed for their trends using the Mann–Kendall (MK) trend test method [55, 56]. Z-value was used to detect whether a statistically significant trend existed. A positive Z-value shows an increasing trend in the time series, whereas a negative Z-value indicates a falling trend. In this study, significance (p-value) thresholds of 0.01 (high), 0.05 (medium), and 0.1 (low) were applied.

2.4.3 Evaluating the impact of changes on water availability

As an indicator of the impact of LULC change on water availability in the study area, daily observed streamflow data were used from May 1957 to June 2012. Since missing values constituted 32 percent of the data, the Mann–Kendall test used the period from

1996 to 2012. However, data from 1957 was also used to observe the general trend of the time series plot.

In addition, the computed actual evapotranspiration (AET) based on Eq. 3 from the TM-WB model was used to evaluate its trend and, at the same time, compared with the FAO WaPOR reanalysis data to evaluate any similarity in temporal trend between the two datasets. We also checked the linear correlation R^2 between TM-WB and WaPOR AET. The second release, with a spatial resolution of 100 m (Level II dataset), was used to obtain the annual time series of the spatial average actual evapotranspiration from FAO WaPOR reanalysis data from 2009 to 2022. This time series was also evaluated for its trend to assess how LULC change affects water availability. We created an AET spatial map for 2009 and 2022 to compare the two years and examine how AET changes with land use. It is important to note that, as highlighted by Blatchford et al. [57], WaPOR data tend to overestimate AET, particularly under certain land cover and climatic conditions. Therefore, this study used the WaPOR dataset primarily for trend analysis rather than for absolute quantification of evapotranspiration, focusing on detecting relative changes over time rather than precise values.

2.4.4 Statistical analysis

To assess trends and determine the significance of changes in hydro-climatic variables such as precipitation, temperature, streamflow, and actual evapotranspiration, the Mann–Kendall (MK) trend test was applied. This non-parametric test is widely used to detect monotonic trends in time series data without assuming any specific distribution. The Z-value indicates the direction of the trend: a positive Z suggests an increasing trend, while a negative Z indicates a decreasing trend. Statistical significance was evaluated using p-value thresholds of 0.01 (high significance), 0.05 (moderate significance), and 0.10 (low significance). In addition, Sen's slope estimator was used to quantify the magnitude of change per year (e.g., mm/year for rainfall or °C/year for temperature). This combined approach provided a robust analysis of long-term trends and their potential implications for water availability and irrigation planning in the study area. Tables and graphs were created with OriginPro and Microsoft Excel (Fig. 3).

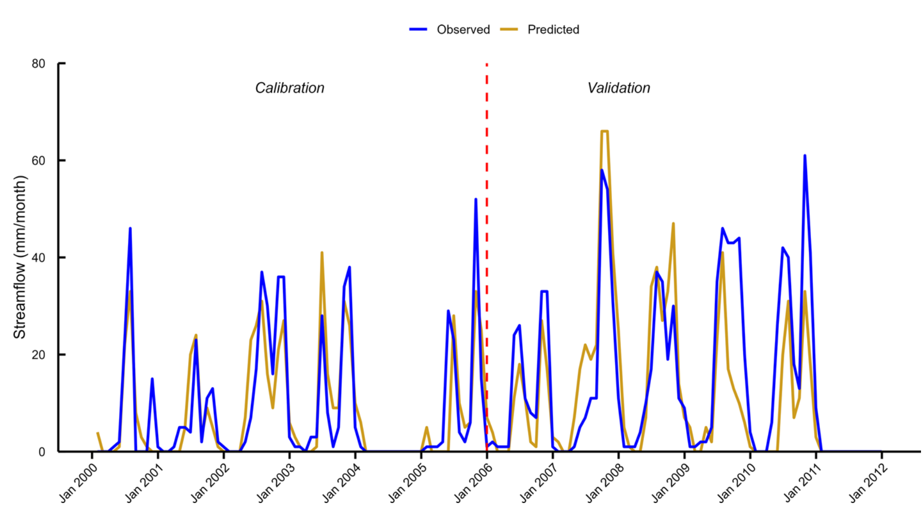

Fig. 3 Observed and predicted streamflow at the Adiembera station in the upper Offin sub-basin in the period from 2001 to 2012

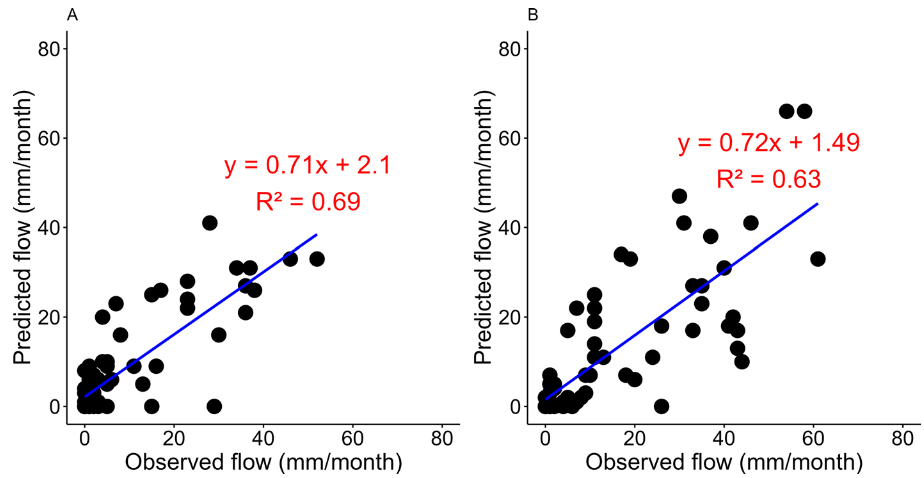

Fig. 4 Scatter plot of measured and predicted monthly flow a) during calibration (2001–2005) and b) during validation (2006–2012)

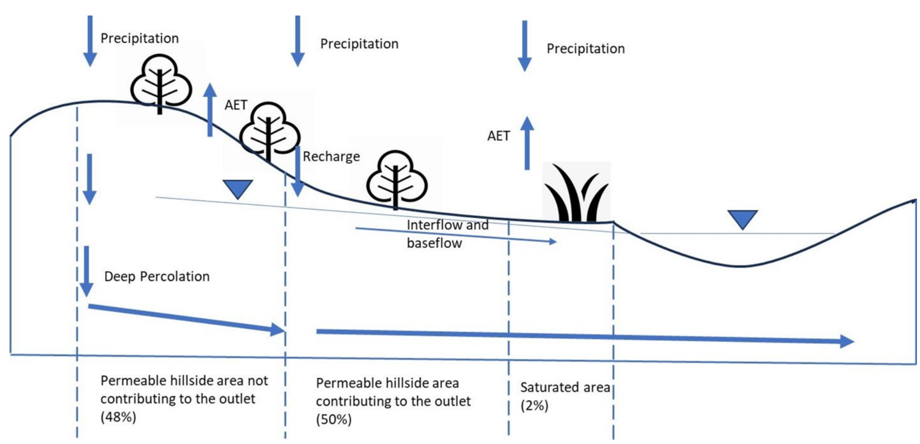

Fig. 5 Conceptual schematic diagram of the Upper Offin landscape and the different landscape units defined for the water balance model

3 Results

3.1 Quantifying the water resources potential

3.1.1 TM-WB modeling

The model generally shows underprediction during rainy periods; in a few cases, there is a mismatch between the recession and rising limbs, which could lead to a mismatch between the major rainfall and runoff events (Fig. 3).

Despite these challenges, the monthly model performance during the calibration period (2000–2005) yielded an R^2 of 0.70, a Nash–Sutcliffe Efficiency (NSE) of 0.70, and a Root Mean Square Error (RMSE) of approximately 7 mm (Fig. 4a, shown only for monthly results). During the validation period (2006–2012), the model maintained satisfactory performance, with an R^2 of 0.63, a NSE of 0.60, and an RMSE of approximately 10 mm (Fig. 4b, shown only for monthly results). These results are considered acceptable for gaining meaningful insights into the components of the water balance.

The sub-basin was conceptually divided into three units in the model (Fig. 5). The detailed model framework can be found in Tilahun et al. [39]. The calibrated parameters for the upper Offin sub-basin (Table 3) indicate that the valley bottom contributes

Table 3 Calibrated parameters of the water balance model for predicting daily and monthly discharge at the outlet of the upper Offin sub-basin

Parameter Notation	Description of the parameter	Unit	Calibrated parameter value
A_s	The portion of the valley bottom saturated area	%	2
A_h	The portion of the hillside area	%	50
$S_{max,s}$	Maximum soil water storage in A_s	Mm	200
$S_{max,h}$	Maximum soil water storage in A_h	Mm	100
Bs_{max}	Maximum storage for base flow linear reservoir	Mm	20
$t_{1/2}$	Base flow half-life time	Days	10
τ_h^*	Interflow from hillside	Days	120
τ_s^*	Interflow from saturated areas	Days	3

Table 4 Long-term average annual Water budget

Water balance components	Average value (mm)	Proportion with Rainfall% %
Rainfall	1329.7	
Stream flow	126.9	9.5
Actual AET	1079.5	81.2
Recharge	126.5	9.5
Deep Percolation	123.4	9.3

flow to the outlet (which accounts for 2% of the total area of the sub-basin). The hillside with good permeability (accounting for 50% of the total area) generates only subsurface flow, not surface runoff (Fig. 5). The remaining 48% does not contribute to the outlet, but evapotranspiration from this area still needs to occur, and likely an additional deep percolation, as unaccounted water, to the outlet (Fig. 5). The maximum soil water storage for the hillsides is relatively small (~ 100 mm), but differs for saturated valley bottom areas (~ 200 mm) due to differences in soil type and slope of the watersheds.

The model's prediction works well when the water from the valley bottom is modified to generate subsurface flow as interflow rather than overland flow. Therefore, on average, three days are required for water to flow out as interflow from this unit to the outlet, while 120 days are needed for the 2nd unit. The longer travel days for interflow from the hillslope are due to the watershed size, whereas the saturated area has a shorter travel time, as it is close to the stream. This combination of parameters yields a better model result.

3.1.2 Water balance components

The TM-WB model was used to extend the monthly flow from 2012 to 2022 and partition the rainwater into streamflow, actual evapotranspiration, recharge, and unaccounted water at the outlet, which is likely to be deep percolation or evapotranspiration (Fig. 5). Table S1 in the Supplementary Material shows each water balance component's annual time series values (baseflow, interflow, recharge, and actual evapotranspiration). Table 4 summarizes the water balance components for the long-term yearly average values and the potential of the water resources.

Generally, the model estimated 126.9 and 126.5 mm of water as streamflow and recharge in the landscape from 2012 to 2022, respectively. Both are 10% of the long-term annual rainfall. This recharge finally becomes streamflow because it is first stored as groundwater in the upper Offin (90 mm) and drains as subsurface flow through baseflow. The remaining amount (37mm) becomes interflow from the valley bottom and hillside as quick flow. Most of the water is lost as evaporation (80%). The unaccounted water at the outlet is 9%, which percolates deep and does not show up at the outlet of the sub-basin. Further study is needed on where it is stored and its flow paths.

3.1.3 The potential for supplemental Irrigation

The long-term average annual streamflow was 126 mm, and the maximum annual flow was 287 mm (Table 2 and Table S1 in the Supplementary Material). We deducted the minimum annual flow (26 mm from Table S1 in Supplementary Material) as ecological flow, and the irrigation potential area based on the available water resources obtained by taking the ratio of these values to the irrigation demand of 525 mm per year (Table S2 in Supplementary Material). This demand is consistent with previous estimates of Radersma and Ridder [50] for Cocoa during the dry period, and this was confirmed during the multi-stakeholder dialogue on cocoa [16]. This is practically possible if a storage structure stores the flows during the rainy period.

During an average year, the maximum irrigable area that can be supported by streamflow becomes 11% of the watershed area. During the wet year, this will reach the maximum area of 30%. The maximum flow is unlikely to occur all the time, but it is included here to illustrate the maximum limit. The temporal distribution within a year needs to be understood and considered to use water from the stream for irrigation directly. Table S3 in the Supplementary Material shows that the minimum flow of 0.005 mm in March was considered to irrigate directly from the stream. The potential becomes less than 1%, which is impractical. The same result was obtained by conducting a flow duration curve analysis from the daily streamflow measurement recorded from 2000 to 2011 at the sub-basin outlet. The 90-percentile flow (flow exceeded 90% of the time) was 0.01mm/day, leading to an irrigation equivalent of 0.24% of the basin.

The feasibility of surface water for a cocoa farm could be a challenge as it is an upland tree. The most practical option is groundwater. The readily available groundwater source from the model is the average baseflow of 100 mm, as shown in Table S1 in the Supplementary Material. The maximum area that can be irrigated from groundwater is approximately 11% of the basin. The baseflow is part of the annual recharge estimated as 126 mm per year in the basin (Table 2).

3.2 Threats from LULC and climate change

3.2.1 Mankran watershed LULC classification

Four LULC maps (Fig. 6) were produced for the Mankran upland watershed for 2008, 2015, 2018, and 2021. The proportion correctly classified (PCC) index and the Kappa statistic, derived from an error matrix, were used to measure classification accuracy. The PCC index was 78%, indicating that 78% of the observations were correctly classified, while the Kappa index was 74.6%, suggesting that the model classification is better than random chance. The overall classification is satisfactory.

As shown in Table 5, in 2008, approximately 82% of the landscape was dominated by forest encompassing dense and sparse vegetation (Fig. 6a). The next dominant land use was food and cash crops from cultivated lands, accounting for 15%. The dominant food crops grown in the area include maize, plantain, yams, and cassava (8.7%), with cash crops such as coffee and citrus (6%) mainly grown on the outskirts of settlements [53]. By the year 2015, significant changes had occurred within the landscape. Agriculture, especially cash crop farming, increased significantly by more than twofold. However,

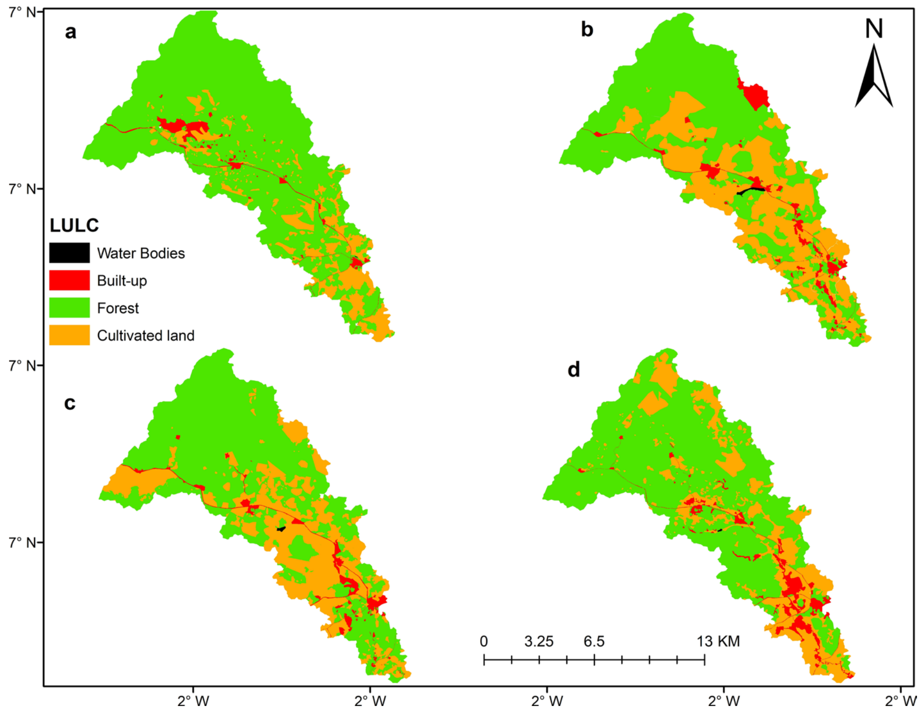

Fig. 6 Land use and Land cover map of the landscape in the Mankran watershed of the upper Offin sub-basin for a) 2008, b) 2015, c) 2018 and d) 2021

Table 5 Land use and Land cover area and proportion of Mankran watershed in Upper Offin sub-basin for 2008, 2015, 2018, and 2021

Year	2008		2015		2018		2021	
	Area (km^2)	(%)	Area (km^2)	(%)	Area (km^2)	(%)	Area (km^2)	(%)
Forest	103.3	82.3	73.8	58.8	80.5	64.2	88.4	70.4
Cultivated land	18.6	14.8	45.8	36.5	40.5	32.3	30.8	24.5
Built-up areas	3.6	2.9	5.9	4.7	4.2	3.3	6.4	5.1
Water Bodies	0.0	0.0	0.0	0.1	0.1	0.3	0.0	0.0

built-up areas and illegal mining activities also made incursions into the southern part of the watershed, where the red spots expanded a lot (Fig. 6b). In 2018, due to the enforcement of anti-illegal mining regulations, the landscape began to recover back to the level of 2008, as shown in Table 5 and Fig. 6c. Thus, the percentage of built-up areas decreased by a factor of two, while forest areas increased by 90%, especially in previously degraded areas that were previously classified as built-up areas. In 2021, the built-up area generally increased, and there was a resurgence of mining in the southern part of the watershed, bringing it back to the level of 2015 (See Table 5 and Fig. 6d). This came in the form of community mining sites where former illegal mining sites were opened to communities to allow them to mine sustainably. This has negatively impacted smallholder farmers by competing with their agricultural lands and soil and water contamination [53].

Boakye et al. [24] have documented the land use change trend for the upper Offin sub-basin. The comparison between the Mankran watershed and the broader upper Offin sub-basin highlights the similarity in trends in land use and land cover changes, but has a different order of magnitude (Fig. 7). Both areas have witnessed reductions in forest cover. Still, the upper Offin Sub-basin experienced a more pronounced decline, dropping

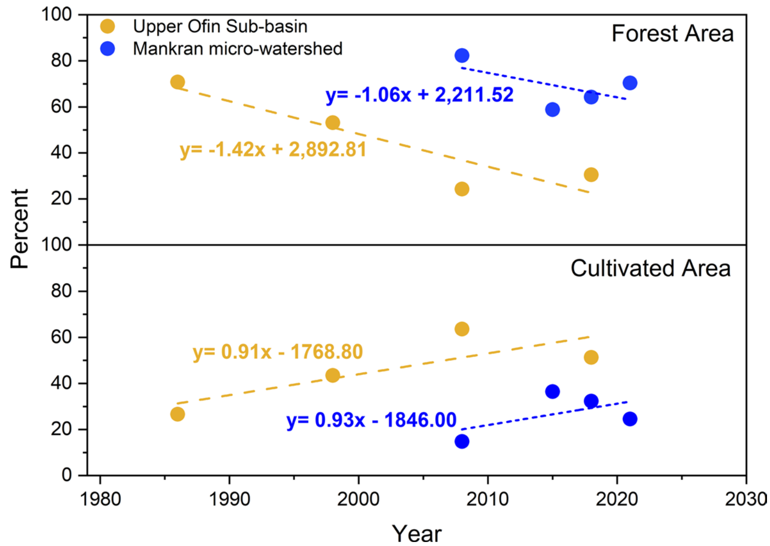

Fig. 7 Forest (upper plot) and cultivated (lower plot) area proportion changes with time in the Mankran watershed in blue and upper Offin in orange dots

from 70% in 1986 to 30% in 2018, while Mankran's forest area decreased from 82% in 2008 to 70% in 2021. Conversely, the trend of cultivated land expansion (Fig. 7) has been similar in both areas, but more pronounced in the upper Offin sub-basin, increasing from 26% in 1986 to 51% in 2018. In contrast, Mankran's cultivated land increased from 15% in 2008 to 25% in 2021. In terms of Built-up areas, both areas experienced an increase, with Mankran doubling its built-up zones from 3 to 5%. In comparison, the upper Offin sub-basins built-up areas increased from 2 to 17%, primarily due to the influence of Kumasi city.

3.2.2 Trend analysis of historical climate variables

Results from Table 4 show no statistically significant increasing trend in annual precipitation from 1981 to 2022. Monthly analyses were also conducted to further investigate seasonal trends. No statistically significant trends (Table 6) were detected for all months except November precipitation, which exhibited a medium, increasing rate at 0.77 mm yr $^{-1}$.

For temperature, it shows that there is a statistically significant increasing trend in maximum and minimum temperature during the period from 1980 to 2022. The strong significant increase rate is 0.03°C and 0.02°C per year for minimum and maximum, respectively. This is consistent with reports from other studies [58].

3.3 Evaluating the impact of changes on water availability

To evaluate whether there is an association between these changes and water availability, we first examined the trend in annual observed streamflow data. The plotted observed streamflow data from the Adiembera station (Fig. 8) shows a significant increase after the end of 1980, with a general decrease from 1957 to 2011. Mann Kendell statistics from 1996 to 2012 showed an increasing slope of 11 mm/year (significant with p-value < 1%).

Then, the trend of AET was evaluated. When the trend of AET generated from the WaPOR dataset and the TM water balance model is examined (Fig. 9), there is a similar pattern of lowering AET across time (Fig. 9), though statistically, it is significant for

Table 6 Mann–Kendall test and Sen's slope estimator results for precipitation and temperature from 1981–2022. Streamflow was from 1996 to 2012

Time Series	s	z	P-value	Slope (mm or °C yr^{-1})
Annual Rainfall	92.25	0.41	0.68	0.93
Monthly Rainfall				
Jan	83	0.89	0.37	0.11
Feb	31	0.32	0.74	0.12
Mar	− 3	− 0.02	0.98	− 0.01
Apr	− 81	− 0.86	0.38	− 0.48
May	− 45	− 0.47	0.63	− 0.19
Jun	77	0.82	0.41	0.48
Jul	− 55	− 0.58	0.56	− 0.42
Aug	− 91	− 0.98	0.33	− 0.5
Sep	57	0.61	0.54	0.63
Oct	141	1.52	0.13	0.9
Nov	**209**	**2.25**	**0.02**	**0.77**
Dec	− 1	0	1	− 0.003
Temperature				
Tmax	**415**	**4.49**	**7.23E-06**	**0.03**
Tmin	**457**	**4.94**	**7.74E-07**	**0.02**
Streamflow				
Annual	**22.2**	**3.37**	**0.00073**	**11.2**
Actual Evapotranspiration (AET)				
AET from WaPOR	**18.3**	**– 2.3**	**0.02**	**– 13.3**
AET from TM-WB	18.3	− 0.3	0.74	− 2.8

Bolded row = significant trend. − decreasing

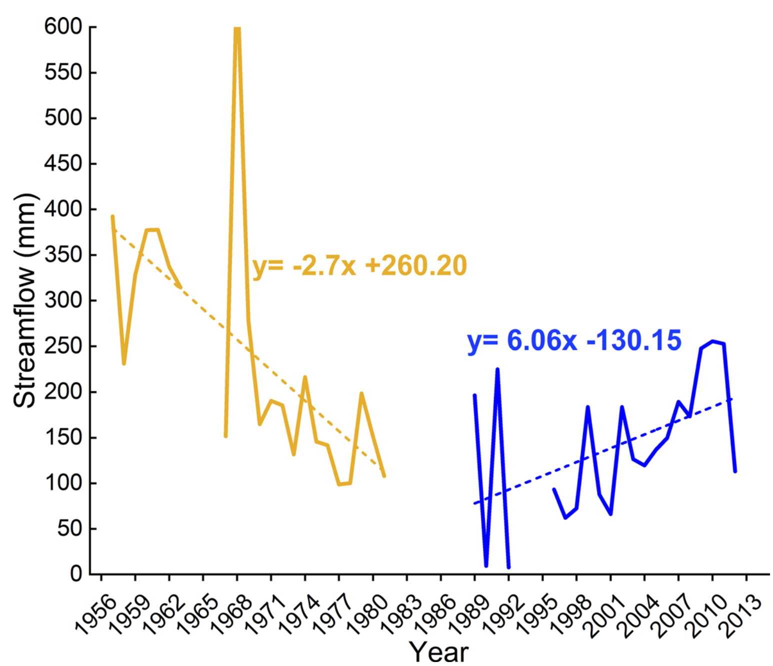

Fig. 8 Streamflow data from 1957 to 2011 with orange color and the streamflow data from 1989 to 2011 with blue color

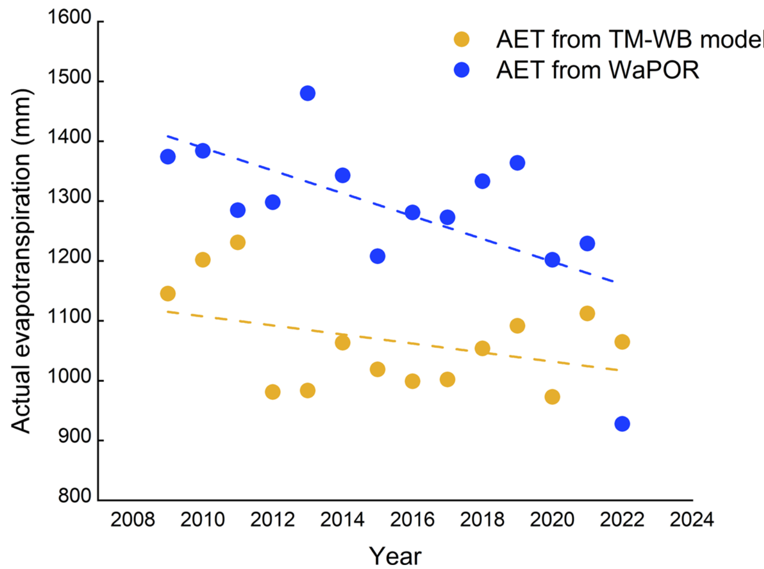

Fig. 9 Time series of actual evapotranspiration from 2008 to 2022 from the water balance model (orange circles) and WaPOR level 2 (blue circles)

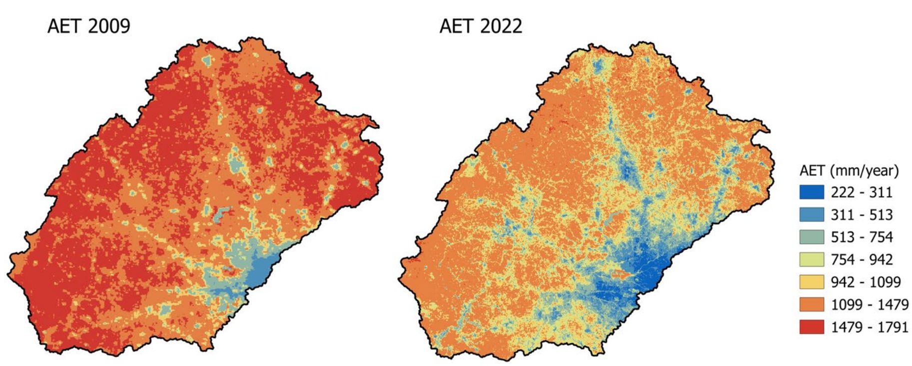

Fig. 10 Spatial distributions of actual ET in the upper Offin sub-basin in 2009 (left) and in 2022 (right)

WaPOR data and non-significant for AET from TM-WB (Table 4). It's worth noting that the WaPOR dataset tends to overestimate AET, with a 14-year average of 1284 mm, compared to the model's 1050 mm. The correlation R^2 between TM-WB and WaPOR AET result is 0.98 by forcing the intercept to zero, indicating its relevance as a data source for evaluating of AET.

The spatial distribution of annual AET from WaPOR for 2009 and 2022 reveals noteworthy variations (Fig. 10). In 2009, the absolute values of actual ET ranged from 311 to 1791 mm, and in 2022, they spanned from 222 to 1479 mm. Despite the overestimation in these absolute values, a general observation is the prevalence of high actual ET in 2009. In the forested regions (depicted in hot red), the spatial average of actual ET was 1457 mm in 2009, diminishing to 1010 mm in 2022 annually. In cultivated lands (depicted in yellow), AET was measured at 1320 mm in 2009 and decreased to 850 mm in 2022, while the built-up areas (in blue) showed that AET values of 733 mm in 2009 and 400 mm in 2022.

4 Discussions

4.1 Potential for supplemental irrigation of Cocoa

The order of magnitude of the model parameters for TM-WB falls within the range reported in the literature for similar landscapes [9, 43]. The high soil water content in the watershed indicates that the landscape is not severely degraded. The area is well-vegetated and covers all-time plants in the year, except in the mining areas, which are less than 5% of the study area [26]. However, it is essential to acknowledge the limitations of underpredicting peak flows, which is likely due to the expansion of runoff-producing areas during longer-duration heavy storms. This expansion is not captured because our model fixes the fraction of streamflow producing areas. Future research should address this limitation by integrating event-based models that can better simulate peak flows.

The estimated groundwater recharge from the water balance (Table 3) in the study area is approximately 2.5 times that of the Volta Basin's groundwater recharge [59]. This study has shown that shallow groundwater recharges (i.e., corresponding with baseflow) account for approximately 10% of the annual rainfall in the Upper-Offin sub-basin. This opens the doors to irrigating up to approximately 10% of the cocoa farm areas in the Upper Offin Basin, which holds the potential to boost cocoa production through supplemental irrigation, especially during dry periods. Assuming the 3 ha of cocoa irrigated area per household, more than 10,000 ha could be irrigated during the dry period using shallow groundwater, and more than 3000 households could benefit from the irrigation.

Additionally, only 52% of the area contributes to the measured discharge and baseflow at the outlet, implying that the remaining 48% of the area may experience deep percolation recharging lower-lying aquifers (Fig. 8). Assuming deep percolation (Table 3) as a potential water source, the possible irrigable area could be more than 20% of the basin land.

However, while this finding holds promise and policy relevance, the practical feasibility of expanding irrigation coverage remains uncertain. Critical issues, such as the economic viability of groundwater abstraction, the sustainability of the water resource under a changing climate and land use, and the infrastructure required for water storage, pumping, and distribution, must be addressed. Moreover, smallholder farmers' financial and technical capacity to adopt and maintain irrigation systems poses significant constraints. Although there is a willingness to invest in irrigation, financial barriers remain a significant constraint to adopting this potential [21]. Therefore, this study only offers a potential land size, realizing this irrigation capacity will depend on targeted investments, institutional support, and further interdisciplinary research into local hydrogeological and socio-economic conditions.

The following section addresses one of the complexities of existing factors, such as climate change interplaying with LULC dynamics in upper Offin, could significantly threaten the potential of water resources to support irrigation [60, 61]. The following section discusses how these changes affect the available water resources.

4.2 Agriculture and Built-up areas increased with time

The study on land use and land cover at the micro-watershed of Mankran (from our research) and its comparison with changes in the upper Offin sub-basin revealed that land use changes were mainly because of agricultural area expansion and illegal mining activities [24, 26]. As shown in Fig. 3A, the general trend of forest area in the last 3

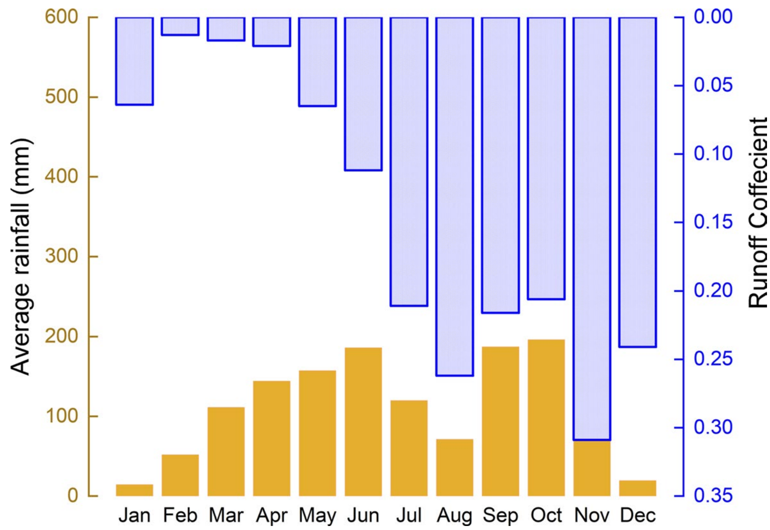

Fig. 11 Average monthly rainfall distribution of the study areas following long-term available data from CHIRPS (1981–2022) and Monthly average runoff coefficient from 2000 to 2011

decades has been decreasing. However, after 2015, the forest area started increasing due to the enforcement of anti-illegal mining regulations, and the landscape began to recover [53]. The analysis of the Mankran micro-watershed area (Table 5) helped to check the validity of previously published reports that highlighted the expansion of agriculture and the built-up areas, mainly for the mining sector, over longer periods in the upper Offin sub-basin [24, 26].

The impact of land use changes in the area is profound, particularly regarding increased sediment yield and its substantial contribution to phosphorus transport [62]. Mining expansion has become prevalent along the river network, resulting in downstream pollution affecting land and water quality [26]. These land use changes, accompanied by mining activities, exert significant adverse effects on the environment and water resources within the study area, even persisting after post-reclamation efforts have been made within the mining sector [8]. As a result, water quality variables, such as total dissolved solids, total phosphate, lead, and arsenic, have consistently exceeded the permissible standards set by the World Health Organization (WHO) in the area [63]. This paper, however, aims to examine the relationship between this land use shift and the impact on the availability of the landscape's water resources.

4.3 LULC changes associated with the trends in streamflow

In this semi-deciduous forest-dominated landscape, LULC changes could potentially impact hydrology. Figure 5 shows a significant increasing trend in streamflow after the end of 1980 associated with the decreasing trend of forest cover and increasing trend of built-up areas and cultivated lands in the area [64, 65]. This is described below by explaining the flow path and how the changes impact the streamflow.

The general increasing coefficient pattern from the dry to the rainy period (Fig. 11) indicates that runoff in the landscape is likely generated because of subsurface storm flow from saturated soil [39]. It was low, only 2%, early in the rainy month of March (Fig. 4). The runoff became 20% of the rainfall at the end of this monsoon season. In August, with minimal rainfall, the coefficient was elevated to 25%, likely due to subsurface flow. The rainfall in March and April first brings the soil to field capacity, and then any excess saturates the watershed, becoming a recharge. The watershed begins responding as subsurface flow during the months of minimum rainfall. The same pattern was followed for the 2nd rainy season, with the coefficient during the rainy months of September and October reaching 20%, while in the dry month of November, it increased to 30%. The fact that the water balance model (Fig. 2, based on soil moisture status and evapotranspiration) fits the streamflow data more closely also suggests that subsurface storm flow or saturation during storm events is likely more dominant than infiltration excess. However, future research is needed to compare infiltration capacity with rainfall intensity and monitor piezometric water level.

The clearing of forest areas and the increase of agriculture and built-up areas tend to change the soil water storage and evapotranspiration dynamics, which could inherently increase the quick flow from the basin through interflow. In this forest area, most rainwater evaporates into the atmosphere, and the remaining infiltrates into the soil [66]. Forest soils are typically rich in organic matter and have a more porous structure due to tree roots and decaying plant material, allowing for better water absorption, storage within the soil, and flow out as baseflow. When agriculture and built-up areas increase, evapotranspiration decreases, and the extra water from the balance flows out quickly from the basin through interflow. The increase in flow over time in the study is consistent with the results from Awotwi et al. [25], who reported a decrease in runoff from 1970 to 1985 and an increasing trend from 1985 to 2010 in the Lower Pra Basin. Anthropogenic activities, such as alluvial mining and the expansion of built-up areas in the basin, are likely causes of the increasing streamflow trend in recent times [8].

4.4 A decrease in actual evapotranspiration associated with LULC impact

The trend in Fig. 9 indicates the decreasing AET, largely attributable to the progressive loss of forested areas, which traditionally facilitate substantial water evaporation through deep-rooted vegetation. The result from WaPOR product is, however, higher than the AET from the TM-WB model. The overestimation by WaPOR is identified by other researchers [57], but the decreasing trend is similar between the two approaches, implying that the land use change is decreasing ET. This trend underscores the potential association of land use changes with AET changes within the basin. The shared declining trend between the model and WaPOR strongly implies a connection between decreasing AET and evolving land use patterns, a correlation previously reported by Awotwi et al. [8] in the Pra Basin using SWAT modeling.

Of particular interest is the spatial alignment of actual ET with the land use patterns within the basin (as depicted in Fig. 10). The high rates of actual ET in forested areas can be attributed to the substantial water storage in the soil and the transpiration of water from deep soil layers. This decrease in actual ET corresponds to a surplus of water that either contributes to runoff or deep percolation within the basin, further emphasizing the influence of land use changes on AET and water dynamics.

4.5 The implication of the study

In Ghana, particularly in this study area, irrigation is an important practice at the valley bottoms and flood plains through individual initiatives and through the Ghana Irrigation Development Authority (GIDA) to produce fruits, vegetables, cereals, and other cash crops [52]. Ghana Cocoa Board has also initiated an irrigation program for farmers in this area from groundwater [16]. The implications of this study for the initiative by COCOBOD are discussed below.

In contrast to Akpoti et al. [23], who focused on spatial groundwater availability through multi-criteria analysis, our results provide a quantitative assessment of water balance components critical to irrigation planning. Moreover, unlike Boakye et al. [24], who emphasized land cover dynamics, we demonstrate how these changes affect water availability, thus offering a more holistic and decision-relevant understanding of irrigation feasibility in cocoa agroforestry systems.

This study observed a rising temperature trend, which, combined with an increase in consecutive dry days reported in recent research on cocoa climate risk in Côte d'Ivoire and Ghana [13], signals a growing climate stress on water availability. These climatic shifts heighten the urgency for sustainable irrigation interventions.

The potential for water resources implies that implementing irrigation from groundwater presents a feasible and innovative solution for irrigated cocoa production in Ghana [67]. Integrating these measures with good agricultural practices, water-saving technologies like micro-sprinklers, access to financing, and farmer training holds significant potential to enhance both water and crop productivity, thereby promoting the sustainability and efficiency of cocoa farming in the region. However, these actions should consider the threats from land use and climate change.

The study identifies associations between land cover change and water balance shifts, which may not be casual. Streamflow and evapotranspiration dynamics are integral parameters governing water balance that are affected by landscape changes [68]. According to Brown et al. [66], increasing the forest cover of a watershed could be associated with a decrease in the total flow volume. In the upper Offin sub-basin, we observe that streamflow has increased while evapotranspiration has decreased, indicating a significant reallocation of water fluxes within the system. This pattern suggests a temporary reduction in water availability for local use, including irrigation, and reflects how land use shifts could be associated with hydrological alteration.

These trends are consistent with findings by Fenta et al. (2025), who demonstrated that the expansion of Eucalyptus plantations in a humid Ethiopian highland watershed led to hydrological changes: decreased streamflow and increased evapotranspiration. Their study confirmed that land cover transitions, especially those involving deep-rooted forest species or vegetation removal, can dramatically alter catchment-scale hydrology by increasing interception and transpiration while decreasing surface runoff. Similarly, in our study area, reducing vegetative cover from forest to other land uses such as agricultural and built-up areas has reduced infiltration and transpiration capacity, resulting in more surface runoff and higher streamflow volumes [69]. Moreover, mining activities have been shown to significantly disrupt hydrological processes through vegetation clearance, soil compaction, and altered drainage patterns, contributing to increased surface runoff and sedimentation [26].

Additionally, a significant decrease in forest areas due to agricultural and built-up area expansion threatens biodiversity and disrupts natural ecosystems. The declines in annual ET are spatially distributed with storage losses, providing insight into the occurrence of vegetative cover conversions. If the current scenario continues, the potential of water resources will diminish with time, with the increasing climate change (as shown in Table

6 in increasing temperature) and anthropogenic activities. The effects of these land use changes may necessitate careful management and conservation through inclusive landscape management efforts to ensure that the available water resources are effectively harnessed for sustainable irrigation. This underscores the importance of holistic and sustainable land and water resource management practices to maximize the irrigation potential of the evolving landscape. However, more research is needed to address the limitations of this study.

The limitations of this study primarily stem from its reliance on remote sensing, which may not capture the full complexity of water resource dynamics and land use changes in the upper Offin basin. While the study provides valuable insights into water balance components and irrigation potential, the lack of continuous observed data for precipitation, temperature, and streamflow affects the accuracy of the water balance assessment. The study acknowledges that deep percolation, which accounts for unmeasured water, requires further investigation to understand its implications for irrigation planning. Moreover, the localized focus on the Upper Offin basin may limit the generalizability of the findings to other areas with different climatic, hydrological, and land use characteristics. The anthropogenic activities affecting water resources, such as illegal mining and extensive agricultural expansion, were only addressed conceptually but not fully with a mechanistic approach. A broader spatio-temporal, physically based model that accounts for mining could enhance the understanding of water resource dynamics in such a landscape. This would facilitate more robust irrigation strategies and sustainable land management practices tailored to local conditions and challenges.

5 Conclusions

The dependence of cocoa farming on the rainfed system is increasingly becoming a challenge in its productivity due to climate change. This concern has initiated the need for supplemental irrigation, especially during dry periods. The study's findings show that shallow groundwater could support supplemental irrigation of approximately 10% of the cocoa farms in the Upper Offin Sub-basin. If deep percolation is considered, the proportional area of the basin to be irrigated could increase to 20% of the sub-basin. This presents a significant opportunity for cocoa and other crop irrigation farms during dry periods. This estimation could give a first insight into the potential and be used for planning purposes with further research in the cocoa-producing region of Ghana. However, a changing landscape characterized by expanding cultivated lands, including urban development and mining activities, threatens this potential. Concurrently, these transformations have shown a clear association of land use change and hydrological changes through streamflow increases and decreases of evapotranspiration. However, further research is imperative to trace the pathways of deep percolation and ascertain its feasibility for irrigation purposes and how it is affected by these changes. In conclusion, the study recommends that water resources have the potential to benefit farmers through supplemental irrigation, which needs the attention of policymakers on how to incentivize farmers to adopt irrigation technologies and ensure they have access to the necessary agricultural inputs to implement these practices successfully. At the same time, there should be a proactive approach to land and water resource management through innovative and integrated landscape management strategies to capitalize on potential.

Policymakers should prioritize sustainability to ensure the long-term development of irrigation in the changing agro-forestry landscapes of West Africa.

Supplementary Information

The online version contains supplementary material available at https://doi.org/10.1007/s43621-025-01794-6.

Supplementary Material

Acknowledgements

This work was carried out under the CGIAR Scaling for Impact Program and the CGIAR Initiative on West and Central African Food Systems Transformation, which is grateful for the support of CGIAR Trust Fund contributors (www.cgiar.org/funders). To learn more about these and other initiatives in the CGIAR research portfolio, visit https://www.cgiar.org/research/cgiar-portfolio/. The authors also acknowledge the invaluable contributions of the Ghana Hydrological Authority for streamflow data used in this study.

Author contributions

Conceptualization, S.A.T and O.C.; Data curation, S.A.T. and S.D.; Formal analysis, S.A.T.; Investigation, S.A.T; Methodology, S.A.T., A.K.A and G.A.; Resources, T.M. and O.C.; Supervision, T.M., and O.C.; Validation, T.M. and M.D.; Writing—original draft, S.A.T and A.K.A.; Writing—review & editing, S.A.T., A.K.A., G.A., B.Z.B., M.D., S.D., T.M. and O.C.; funding acquisition, O.C. All authors have read and agreed to the published version of the manuscript.

Funding

This research was funded by the CGIAR Scaling for Impact Program and CGIAR Regional Initiative on West and Central African Food Systems Transformation, which is grateful for the support of CGIAR Trust Fund contributors (www.cgiar.org/funders).

Data availability

The datasets generated during and/or analysed during the current study are available from the corresponding author on reasonable request.

Declarations

Ethics approval and consent to participate

Not Applicable.

Consent to Participate

Not Applicable.

Consent to Publication

Not Applicable.

Competing interest

The authors declare no competing interests.

Received: 20 January 2025 / Accepted: 11 August 2025

Published online: 28 August 2025

References

1. African Development Bank Group (AfDB). Tracking Africa's progress in figures. 2014. https://www.afdb.org/fileadmin/uploads/afdb/Documents/Publications/Tracking_Africa's_Progress_in_Figures.pdf
2. Potapov P, Turubanova S, Hansen MC, Tyukavina A, Zalles V, Khan A, et al. Global maps of cropland extent and change show accelerated cropland expansion in the twenty-first century. Nature Food. 2022;3(1):19–28. https://doi.org/10.1038/s43016-021-00429-z.
3. Ussiri DA, Lal R. Soil degradation in sub-Saharan Africa: Challenges and opportunities for restoration. Soil Degrad Restorat Africa, 2019, pp.1–24.
4. Keenan RJ, Reams GA, Achard F, de Freitas JV, Grainger A, Lindquist E. Dynamics of global forest area: results from the FAO Global Forest Resources Assessment 2015. For Ecol Manage. 2015;352:9–20. https://doi.org/10.1016/j.foreco.2015.06.014.
5. Emediegwu LE, Wossink A, Hall A. The impacts of climate change on agriculture in sub-Saharan Africa: a spatial panel data approach. World Dev. 2022;158: 105967. https://doi.org/10.1016/j.worlddev.2022.105967.
6. Zougmoré RB, Läderach P, Campbell BM. Transforming food systems in Africa under climate change pressure: Role of climate-smart agriculture. Sustainability. 2021;13(8):4305. https://doi.org/10.3390/su13084305.
7. Lal R. Food security in a changing climate. Ecohydrol Hydrobiol. 2013;13(1):8–21. https://doi.org/10.1016/j.ecohyd.2013.03.006.
8. Awotwi A, Anornu GK, Quaye-Ballard JA, Annor T, Forkuo EK, Harris E, et al. Water balance responses to land-use/land-cover changes in the Pra River Basin of Ghana, 1986–2025. CATENA. 2019;182: 104129. https://doi.org/10.1016/j.catena.2019.104129.
9. Christiansen E, Awadzi TW. Water balance in a moist semi-deciduous forest in Ghana. West African J Appl Ecol. 2000;1(1):11–22.

10. Sigopi M, Shoko C, Dube T. Advancements in remote sensing technologies for accurate monitoring and management of surface water resources in Africa: an overview, limitations, and future directions. Geocarto Int. 2024;39(1):2347935. https://doi.org/10.1080/10106049.2024.2347935.
11. Nyamekye AP, Tian Z, Cheng F. Analysis on the contribution of agricultural sector on the economic development of Ghana. Open J Bus Manage. 2021;9:1297–311. https://doi.org/10.4236/ojbm.2021.93070.
12. Wainaina P, Minang PA, Duguma L, Muthee K. A review of the trade-offs across different cocoa production systems in Ghana. Sustainability. 2021;13:10945. https://doi.org/10.3390/su131910945.
13. Obahoundje S, Akpoti K, Zwart SJ, Tilahun S, Cofie O. Implications of changes in water stress and precipitation extremes for cocoa production in Côte D'Ivoire and Ghana. Int J Climatol. 2025. https://doi.org/10.1002/joc.8872.
14. Serdeczny O, Adams S, Baarsch F, Coumou D, Robinson A, Hare W, Schaeffer M, Perrette M, Reinhardt J. Climate change impacts in Sub-Saharan Africa: from physical changes to their social repercussions. Reg Environ Change. 2017;17:1585–600. https://doi.org/10.1007/s10113-015-0910-2.
15. Koide J, Yokoyama S, Hirouchi S, Hirose C, Oka N, Oda M, Yanagihara S. Exploring climate-resilient and risk-efficient cropping strategies using a new pond irrigation system: an experimental study in northern Ghana. Agric Syst. 2021;191: 103149. https://doi.org/10.1016/j.agsy.2021.103149.
16. Ofosu A, Minh TT. Small-Scale Irrigation Dialogue Space: Understanding the scalability of solar-powered irrigation in Ghana: market segmentation and mapping pump suitability. 2021. https://cgspace.cgiar.org/bitstream/handle/10568/114252/SScale_irrigation_0707.pdf?sequence=1%26isAllowed=y
17. Gebrezgabher S, Leh M, Merrey DJ, Kodua TT, Schmitter P. Solar photovoltaic technology for small-scale irrigation in Ghana: suitability mapping and business models. In: Agricultural water management–making a business case for smallholders (vol. 178). International Water Management Institute (IWMI). 2021. https://doi.org/10.5337/2021.209
18. Xie H, You L, Wielgosz B, Ringler C. Estimating the potential for expanding smallholder irrigation in Sub-Saharan Africa. Agric Water Manag. 2014;131:183–93. https://doi.org/10.1016/j.agwat.2013.08.011.
19. Cocoa Post. Ghana Cocoa Board hands over the first solar irrigation system to a farmer. Retrieved May 16, 2019, 17-08-2023, 2019.
20. Tilahun SA, Gbodji KK, Minh TT, Mabhaudhi T, Cofie O. Peter Oppong's inspiring journey: smallholder farmers like Oppong are reaping the benefits of solar-powered irrigation, a cost-effective and easy-to-implement technology. Colombo, Sri Lanka: International Water Management Institute (IWMI), 2023.
21. Gbodji KK, Quarmine W, Minh TT. Effective demand for climate-smart adaptation: a case of solar technologies for cocoa irrigation in Ghana. Sustain Environ. 2023;9:2258472. https://doi.org/10.1080/27658511.2023.2258472.
22. Amponsah-Doku B, Daymond A, Robinson S, Atuah L, Sizmur T. Improving soil health and closing the yield gap of cocoa production in Ghana: a review. Sci African. 2022;15:e01075. https://doi.org/10.1016/j.sciaf.2021.e01075.
23. Akpoti K, Dembélé M, Forkuor G, Obuobie E, Mabhaudhi T, Cofie O. Integrating GIS and remote sensing for land use/land cover mapping and groundwater potential assessment for climate-smart cocoa irrigation in Ghana. Sci Rep. 2023;13(1):16025. https://doi.org/10.1038/s41598-023-43286-5.
24. Boakye E, Anyemedu FOK, Quaye-Ballard JA, Donkor EA. Spatio-temporal analysis of land use/cover changes in the Pra River Basin, Ghana. Applied Geomatics. 2020;12:83–93. https://doi.org/10.1007/s12518-019-00278-3.
25. Awotwi A, Anornu GK, Quaye-Ballard J, Annor T, Forkuo EK. Analysis of climate and anthropogenic impacts on runoff in the Lower Pra River Basin of Ghana. Heliyon. 2017. https://doi.org/10.1016/j.heliyon.2017.e00477.
26. Snapir B, Simms DM, Waine TW. Mapping the expansion of galamsey gold mines in the cocoa growing area of Ghana using optical remote sensing. Int J Appl Earth Obs Geoinf. 2017;58:225–33. https://doi.org/10.1016/j.jag.2017.02.009.
27. Awotwi A, Anornu GK, Quaye-Ballard JA, Annor T, Nti IK, Odai SN, et al. Impact of post-reclamation of soil by large-scale, small-scale and illegal mining on water balance components and sediment yield: Pra River Basin case study. Soil Tillage Res. 2021;211:105026. https://doi.org/10.1016/j.still.2021.105026.
28. Anani CY, Anim RO, Armah BN, Atichogbe JF, Sakyi PA, Mahu E, Asiedu DK. Petrography of detrital zircons from sandstones of the Lower Devonian Accraian Formation, SE Ghana: Implications on provenance. Geol J. 2020;55(5):3716–31. https://doi.org/10.1002/gj.3633.
29. Smith AJ, Henry G, Frost-Killian S. A review of the Birimian Supergroup-and Tarkwaian Group-hosted gold deposits of Ghana. Episod J Int Geosci. 2016;39(2):177–97. https://doi.org/10.18814/epiiugs/2016/v39i2/95775.
30. Appiah-Adjei EK, Osei-Nuamah I. Hydrogeological evaluation of geological formations in Ashanti Region Ghana. J Sci Technol (Ghana). 2017;37(1):34–50. https://doi.org/10.4314/just.v37i1.4.
31. Hengl T. Soil texture classes (USDA system) for 6 soil depths (0, 10, 30, 60, 100 and 200 cm) at 250 m (v0.2). Zenodo. 2018. https://doi.org/10.5281/zenodo.2525817
32. Zhang X, Liu L, Chen X, Gao Y, Xie S, Mi J. GLC_FCS30: Global land-cover product with fine classification system at 30 m using time-series Landsat imagery. Earth Syst Sci Data. 2021;13(6):2753–76. https://doi.org/10.5194/essd-13-2753-2021.
33. Abu IO, Szantoi Z, Brink A, Robuchon M, Thiel M. Detecting cocoa plantations in Côte d'Ivoire and Ghana and their implications on protected areas. Ecol Ind. 2021;129: 107863. https://doi.org/10.1016/j.ecolind.2021.107863.
34. Dickson K, Benneh G. A new geography of Ghana. New York: Longman; 1995. p. 21–33.
35. Kusimi JM, Yiran GA, Attua EM. Soil erosion and sediment yield modelling in the Pra River Basin of Ghana using the Revised Universal Soil Loss Equation (RUSLE). Ghana J Geograph. 2015;7(2):38–57.
36. Krysanova V, Hattermann F, Huang S, Hesse C, Vetter T, Liersch S, Koch H, Kundzewicz ZW. Modelling climate and land-use change impacts with SWIM: lessons learnt from multiple applications. Hydrol Sci J. 2015;60(4):606–35.
37. Steenhuis TS, Collick AS, Easton ZM, Leggesse ES, Bayabil HK, White ED, Awulachew SB, Adgo E, Ahmed AA. Predicting discharge and sediment for the Abay (Blue Nile) with a simple model. Hydrol Process. 2009;23:3728–37. https://doi.org/10.1002/hyp.7513.
38. Tilahun SA, Guzman CD, Zegeye AD, Engda TA, Collick AS, Rimmer A, Steenhuis TS. An efficient semi-distributed hillslope erosion model for the subhumid Ethiopian Highlands. Hydrol Earth Syst Sci. 2013;17(3):1051–63. https://doi.org/10.5194/hess-17-1051-2013.
39. Tilahun SA, Guzman CD, Zegeye AD, Dagnew DC, Collick AS, Yitaferu B, Steenhuis TS. Distributed discharge and sediment concentration predictions in the sub-humid Ethiopian highlands: the Debre Mawi watershed. Hydrol Process. 2015;29(7):1817–28. https://doi.org/10.1002/hyp.10298.

40. Taylor JC, van de Giesen N, Steenhuis TS. West Africa: Volta discharge data quality assessment and use 1. JAWRA J Am Water Resour Assoc. 2006;42(4):1113–26. https://doi.org/10.1111/j.1752-1688.2006.tb04517.x.
41. Alemie TC, Tilahun SA, Ochoa-Tocachi BF, Schmitter P, Buytaert W, Parlange JY, Steenhuis TS. Predicting shallow groundwater tables for sloping highland aquifers. Water Resour Res. 2019;55(12):11088–100. https://doi.org/10.1029/2019WR025050.
42. Hargreaves GH, Samani ZA. Reference crop evapotranspiration from temperature. Appl Eng Agric. 1985;1(2):96–9. https://doi.org/10.13031/2013.26773.
43. Obalum SE, Nwite JC, Oppong J, Igwe CA, Wakatsuki T. Variations in selected soil physical properties with landforms and slope within an inland valley ecosystem in Ashanti Region of Ghana. Soil Water Res. 2011;6(2):73–82. https://doi.org/10.17221/17/2010-SWR.
44. Funk C, Peterson P, Landsfeld M, Pedreros D, Verdin J, Shukla S, et al. The climate hazards infrared precipitation with stations—a new environmental record for monitoring extremes. Sci Data. 2015;2(1):1–21. https://doi.org/10.1038/sdata.2015.66.
45. Atiah WA, Tsidu GM, Amekudzi LK. Investigating the merits of gauge and satellite rainfall data at local scales in Ghana. West Africa Weather Clim Extremes. 2020;30: 100292. https://doi.org/10.1016/j.wace.2020.100292.
46. Hersbach H, Bell B, Berrisford P, Hirahara S, Horányi A, Muñoz-Sabater J, et al. The ERA5 global reanalysis. Q J R Meteorol Soc. 2020;146(730):1999–2049. https://doi.org/10.1002/qj.3803.
47. Randles CA, Da Silva AM, Buchard V, Colarco PR, Darmenov A, Govindaraju R, et al. The MERRA-2 aerosol reanalysis, 1980 onward Part I: System description and data assimilation evaluation. J Clim. 2017;30(17):6823–50. https://doi.org/10.1175/JCLI-D-16-0609.1.
48. Sekyi-Annan E, Tischbein B, Diekkrüger B, Khamzina A. Performance evaluation of reservoir-based irrigation schemes in the Upper East region of Ghana. Agric Water Manag. 2018;202:134–45. https://doi.org/10.1016/j.agwat.2018.02.023.
49. Worqlul AW, Collick AS, Rossiter DG, Langan S, Steenhuis TS. Assessment of surface water irrigation potential in the Ethiopian highlands: The Lake Tana Basin. CATENA. 2015;129:76–85. https://doi.org/10.1016/j.catena.2015.02.020.
50. Radersma S, de Ridder N. Computed evapotranspiration of annual and perennial crops at different temporal and spatial scales using published parameter values. Agric Water Manag. 1996;31(1–2):17–34.
51. Allen RG, Pereira LS, Raes D, Smith M. Crop evapotranspiration-Guidelines for computing crop water requirements-FAO Irrigation and drainage paper 56. Fao Rome. 1998;300(9):D05109.
52. Agodzo SK, Bessah E, Nyatuame M. A review of the water resources of Ghana in a changing climate and anthropogenic stresses. Front Water. 2023;4:973825. https://doi.org/10.3389/frwa.2022.973825.
53. Atampugre G, Mensah E, Boateng E, Mabhaudhi T, Cofie O. Situational analysis of a social-ecological landscape in Ghana's Ahafo Ano Southwest District. Colombo, Sri Lanka: International Water Management Institute (IWMI). CGIAR Initiative on West and Central African Food Systems Transformation. 2022; 57p.
54. Lillesand T, Kiefer RW, Chipman J. Remote sensing and image interpretation. Wiley; 2015.
55. Mann HB. Nonparametric tests against trend. Econometrica J Econom Soc. 1945. https://doi.org/10.2307/1907187.
56. Yue S, Wang CY. Regional streamflow trend detection with consideration of both temporal and spatial correlation. Int J Climatol A J Royal Meteorol Soc. 2002;22(8):933–46. https://doi.org/10.1002/joc.781.
57. Blatchford ML, Mannaerts CM, Njuki SM, Nouri H, Zeng Y, Pelgrum H, et al. Evaluation of WaPOR V2 evapotranspiration products across Africa. Hydrol Process. 2020;34(15):3200–21. https://doi.org/10.1002/hyp.13791.
58. Lavin Montero AM. Climatic changes in temperature and salinity in the subtropical North Atlantic (Doctoral dissertation, Massachusetts Institute of Technology), 1993
59. Obuobie E, Diekkrueger B, Agyekum W, Agodzo S. Groundwater level monitoring and recharge estimation in the White Volta River basin of Ghana. J Afr Earth Sc. 2012;71:80–6. https://doi.org/10.1016/j.jafrearsci.2012.06.005.
60. Daba MH, You S. Quantitatively assessing the future land-use/land-cover changes and their driving factors in the upper stream of the Awash River based on the CA–markov model and their implications for water resources management. Sustainability. 2022;14(3):1538. https://doi.org/10.3390/su14031538.
61. Näschen K, Diekkrüger B, Evers M, Höllermann B, Steinbach S, Thonfeld F. The impact of land use/land cover change (LULCC) on water resources in a tropical catchment in Tanzania under different climate change scenarios. Sustainability. 2019;11(24):7083. https://doi.org/10.3390/su11247083.
62. Akrasi SA, Ansa-Asare OD. Assessing sediment and nutrient transport in the Pra Basin of Ghana. West African J Appl Ecol. 2008;13(1):45–54. https://doi.org/10.4314/wajae.v13i1.40583.
63. Bessah E, Raji AO, Taiwo OJ, Agodzo SK, Ololade OO, Strapasson A, Donkor E. Assessment of surface waters and pollution impacts in Southern Ghana. Hydrol Res. 2021;52(6):1423–35. https://doi.org/10.2166/nh.2021.051.
64. Babar S, Ramesh H. Streamflow response to land use–land cover change over the Nethravathi River Basin. India Journal of Hydrologic Engineering. 2015;20(10):05015002. https://doi.org/10.1061/(ASCE)HE.1943-5584.0001177.
65. Mekonnen DF, Duan Z, Rientjes T, Disse M. Analysis of combined and isolated effects of land-use and land-cover changes and climate change on the upper Blue Nile River basin's streamflow. Hydrol Earth Syst Sci. 2018;22(12):6187–207. https://doi.org/10.5194/hess-22-6187-2018.
66. Brown AE, Western AW, McMahon TA, Zhang L. Impact of forest cover changes on annual streamflow and flow duration curves. J Hydrol. 2013;483:39–50. https://doi.org/10.1016/j.jhydrol.2012.12.031.
67. Minh TT, Ofosu A. Solar-based irrigation bundle profile and scaling in Ghana. Colombo, Sri Lanka: International Water Management Institute (IWMI). CGIAR Initiative on mixed farming systems. 2022, 27p. https://cgspace.cgiar.org/bitstreams/1ef12ede-adfe-49e0-946e-55c9178ad0b8/download
68. Heerspink BP, Kendall AD, Coe MT, Hyndman DW. Trends in streamflow, evapotranspiration, and groundwater storage across the Amazon Basin linked to changing precipitation and land cover. J Hydrol Region Stud. 2020;32: 100755. https://doi.org/10.1016/j.ejrh.2020.100755.
69. Achugbu IC, Olufayo AA, Balogun IA, Dudhia J, McAllister M, Adefisan EA, Naabil E. Potential effects of land use land cover change on streamflow over the Sokoto Rima River Basin. Heliyon. 2022. https://doi.org/10.1016/j.heliyon.2022.e09779.

Publisher's Note